



## Pharmaceutical Biotechnology

# Vascular Endothelial Growth Factor–Releasing Microspheres Based on Poly( $\epsilon$ -Caprolactone-PEG- $\epsilon$ -Caprolactone)-*b*-Poly(L-Lactide) Multiblock Copolymers Incorporated in a Three-Dimensional Printed Poly(Dimethylsiloxane) Cell Macroencapsulation Device



Karina C. Scheiner<sup>1</sup>, Fergal Coulter<sup>2,3</sup>, Roel F. Maas-Bakker<sup>1</sup>, Giulio Gherzi<sup>4,5</sup>, Thanh T. Nguyen<sup>6</sup>, Rob Steendam<sup>6</sup>, Garry P. Duffy<sup>7</sup>, Wim E. Hennink<sup>1</sup>, Eoin D. O’Cearbhaill<sup>2</sup>, Robbert J. Kok<sup>1,\*</sup>

<sup>1</sup> Department of Pharmaceutics, Utrecht Institute of Pharmaceutical Sciences, Utrecht University, Universiteitsweg 99, 3584 CG Utrecht, The Netherlands

<sup>2</sup> UCD Centre for Biomedical Engineering, School of Mechanical and Materials Engineering, University College Dublin, Engineering Building Belfield Dublin 4, Dublin, Ireland

<sup>3</sup> Department of Complex Materials, ETH Zurich, Vladimir-Prelog-Weg 1-5/10, 8093 Zürich, Switzerland

<sup>4</sup> Abiel srl, ARCA Incubatore di Imprese, viale delle Scienze Ed.16, 90128 Palermo, Italy

<sup>5</sup> Dipartimento di Scienze e Tecnologie Biologiche Chimiche e Farmaceutiche, Università degli Studi di Palermo, viale delle Scienze Ed.16, 90128 Palermo, Italy

<sup>6</sup> InnoCore Pharmaceuticals B.V., L.J. Zielstraweg 1, 9713 GX Groningen, The Netherlands

<sup>7</sup> Discipline of Anatomy, School of Medicine, National University of Ireland Galway, University Road, Galway, Ireland

## ARTICLE INFO

## Article history:

Received 28 August 2019

Revised 11 October 2019

Accepted 15 October 2019

Available online 22 October 2019

## Keywords:

controlled release

PDMS implants

VEGF

multiblock copolymers

diabetes type 1

artificial pancreas

## ABSTRACT

Pancreatic islet transplantation is a promising advanced therapy that has been used to treat patients suffering from diabetes type 1. Traditionally, pancreatic islets are infused via the portal vein, which is subsequently intended to engraft in the liver. Severe immunosuppressive treatments are necessary, however, to prevent rejection of the transplanted islets. Novel approaches therefore have focused on encapsulation of the islets in biomaterial implants which can protect the islets and offer an organ-like environment. Vascularization of the device’s surface is a prerequisite for the survival and proper functioning of transplanted pancreatic islets. We are pursuing a prevascularization strategy by incorporation of vascular endothelial growth factor (VEGF)-loaded microspheres in 3-dimensional printed poly(dimethylsiloxane)-based devices prior to their prospective loading with transplanted cells. Microspheres (~50  $\mu\text{m}$ ) were based on poly( $\epsilon$ -caprolactone-PEG- $\epsilon$ -caprolactone)-*b*-poly(L-lactide) multiblock copolymers and were loaded with 10  $\mu\text{g}$  VEGF/mg microspheres, and subsequently dispersed in a hyaluronic acid carrier liquid. *In vitro* release studies at 37°C demonstrated continuous release of fully bioactive VEGF for 4 weeks. In conclusion, our results demonstrate that incorporation of VEGF-releasing microspheres ensures adequate release of VEGF for a time window of 4 weeks, which is attractive in view of the vascularization of artificial pancreas implants.

© 2020 American Pharmacists Association®. Published by Elsevier Inc. All rights reserved.

**Abbreviations used:** FITC-HA, fluorescein isothiocyanate-labeled hyaluronic acid; HA, hyaluronic acid; HUVEC, human umbilical vein endothelial cells; IVR, *in vitro* release; PBS, phosphate buffered saline; PCL, poly(caprolactone); PDMS, poly(dimethylsiloxane); PEG, poly(ethylene glycol); PLGA, poly(lactic-co-glycolic acid); VEGF, vascular endothelial growth factor.

This article contains supplementary material available from the authors by request or via the Internet at <https://doi.org/10.1016/j.xphs.2019.10.028>.

\* Correspondence to: Robbert J. Kok (Telephone: +31-620275995).

E-mail address: [r.j.kok@uu.nl](mailto:r.j.kok@uu.nl) (R.J. Kok).

## Introduction

Patients with juvenile diabetes (diabetes type 1) suffer from inadequate insulin production, which often relates to autoimmune destruction of the pancreatic beta-cells.<sup>1</sup> Although blood glucose homeostasis can be restored by injection of insulin, novel advanced therapies are being pursued that can restore insulin production.

Transplantation of healthy insulin-secreting pancreatic islets is a promising treatment for diabetes type 1 that has been studied since the 1960s.<sup>2</sup> Traditionally, pancreatic islets are infused into the portal vein and become engrafted in the microvasculature of the liver. However, poor islet survival, rejection by the host's immune system, and the need to use strong immunosuppressing drugs have restricted this treatment's widespread use.<sup>3</sup> Another issue is the lack of donors for pancreatic islet transplantation which is especially severe because on average 3 donors are needed per recipient.<sup>2,4</sup> Strategies that can improve the efficiency of islet transplantation and the overall survival of islets are therefore warranted. Encapsulating pancreatic islets into a biomaterial device is an attractive approach, as it provides a physical barrier between the transplanted islets and the host's immune cells, creating an immune-deprived organ-like environment.<sup>5</sup> Pancreatic islet encapsulation devices have been developed for subcutaneous implantation and have even advanced into phase I-II clinical testing.<sup>5,6</sup> In some cases, devices are prefilled with islets before implantation while other devices include filling ports, offering islet replenishment.<sup>7</sup> Because the formation of blood vessels is vital for transport of oxygen and nutrients, neovascularization of the device remains the key challenge for survival of pancreatic islets after transplantation<sup>8</sup>; moreover, vascularization of the device is also needed for transport of released insulin into the circulation and beyond.<sup>3,5</sup> Several approaches seem feasible, among others coating of the polymeric implants with compounds such as fibrin and platelet-rich plasma to mimic the extracellular matrix, or coformulation of proangiogenic growth factors within the device,<sup>9,10</sup> for instance, vascular endothelial growth factor (VEGF).<sup>11–13</sup> Proper functional vascularization of the surface of implants, that is, the formation of stable blood vessels that encompass the device, will take around 4 weeks upon implantation, depending on the site of implantation, as shown in rodent models.<sup>10,14,15</sup> We therefore postulate that continuous delivery of VEGF for 3–4 weeks is preferred and that such a sustained release can best be achieved by its encapsulation in a controlled drug delivery system such as microsphere.<sup>16,17</sup> The most commonly used polymer for the preparation of microspheres, poly(lactic-co-glycolic acid) (PLGA),<sup>18–20</sup> has several drawbacks regarding the release profile and stability of encapsulated proteins.<sup>21,22</sup> The release of encapsulated cargo is often biphasic, that is, a high burst release followed by a relatively slow release,<sup>20,23,24</sup> and is thus not a preferred release profile for vascularization of implants.<sup>15,25</sup> Furthermore, the acidic degradation products of PLGA-based systems cause a pH decrease within the polymeric matrix,<sup>26,27</sup> and therefore negatively impact the stability of proteins.<sup>21,28,29</sup> We therefore evaluated a different kind of biodegradable polymer composed of multiblock copolymers with alternating hydrophilic and hydrophobic blocks<sup>30,31</sup> for the encapsulation of VEGF in microspheres. These multiblock copolymers form amorphous domains [primarily consisting of poly( $\epsilon$ -caprolactone)-poly(ethylene glycol)-poly( $\epsilon$ -caprolactone) blocks] and semi-crystalline domains [mainly composed of poly(L-lactic acid) blocks], and are attractive for protein delivery due to their well-controlled swelling properties which allow continuous release through diffusion with low burst release.<sup>32–35</sup> The release of proteins can be tailored by the weight fraction and molecular weight ( $M_w$ ) of poly(ethylene glycol) (PEG),<sup>33,36</sup> which was also demonstrated for microspheres loaded with VEGF.<sup>35</sup> In this study, we incorporated VEGF-loaded microspheres in poly(dimethylsiloxane) (PDMS)-based devices<sup>37</sup> and studied the release of VEGF and its bioactivity. Hyaluronic acid (HA) solution served as carrier liquid for VEGF-loaded microspheres. Both PDMS and HA have been reported as suitable biomaterials for pancreatic islets transplantation systems.<sup>38–40</sup> The current PDMS devices were prepared by 3-dimensional (3D) printing, an arising technology in the

biomaterial field which can produce well-defined reproducible scaffolds.<sup>41</sup> PDMS membranes are highly gas permeable; however, they are also required to facilitate the transportation of larger molecules, such as proteins, for cell microencapsulation applications.<sup>5</sup> Therefore, micrometer-sized pores were created by inclusion of a porogen, which, after its extraction, results in a permeable structure through which VEGF can diffuse into the surrounding fluids. We characterized the devices by scanning electron microscopy (SEM) and studied the distribution of red-labeled microspheres within the device. The *in vitro* release (IVR) of VEGF from PDMS devices filled with VEGF microspheres was studied by ELISA. The bioactivity of released VEGF was demonstrated by a human umbilical vein endothelial cell (HUVEC) proliferation-based bioassay.

## Materials and Methods

### Materials

PDMS devices were prepared by 3D printing using silicone rubber elastomer (PDMS) NuSil MED-4840 (Avantor, Radnor, PA) (F. B. Coulter and E. D. O'Ceirhaill, unpublished data, 2019).<sup>37</sup> Hyaluronic acid (HA) and FITC-HA (fluorescein isothiocyanate-labeled HA) (both 1.26 MDa) were supplied by Contipro (Prague, Czech Republic). Recombinant human VEGF 165 was purchased from PeproTech Inc. (Rocky Hill, NJ). PLGA (50:50, i.v. 0.4 dL/g) was purchased from Corbion (Gorinchem, the Netherlands). Poly(vinyl alcohol) (87%–90% hydrolyzed, average  $M_w$  30,000–70,000), Tween 20, sodium chloride, and fluorescein sodium salt were purchased from Sigma Aldrich (Zwijndrecht, the Netherlands). Dichloromethane was purchased from Biosolve Chimie (Dieuze, France). Blue Dextran 2000 (2 MDa) was purchased from GE Healthcare Bio-Sciences AB (Uppsala, Sweden). Nile Red was purchased from Carl Roth (Karlsruhe, Germany). Gibco® Dulbecco's phosphate-buffered saline (PBS; 10 $\times$ , composition 27 mM KCl, 15 mM H<sub>2</sub>PO<sub>4</sub>, 1.4 M NaCl, 81 mM Na<sub>2</sub>HPO<sub>4</sub>  $\times$  7H<sub>2</sub>O) and propidium iodide were purchased from Thermo Fisher Scientific (Bleiswijk, The Netherlands). Collagen I (from rat tail) was obtained from Corning (Corning, NY). Calcein AM was purchased from Cayman Chemical Company (Ann Arbor, MI).

### Methods

#### Preparation of Study Components

**Preparation of HA-Based Carrier Liquid.** HA was dissolved in 10 mL PBS pH 7.4 (Dulbecco's PBS, final concentration 10 mg/mL) by stirring under mild heating ( $\sim$ 40°C) for 16 h. After complete dissolution (determined visually), the viscous solution was autoclaved (program: 120°C, 2 bar, 21 min, autoclave: Zirbus Technology, Benelux BV, Tiel, The Netherlands) and cooled down to room temperature. HA carrier liquid was stored at 4°C.

**Preparation of Microspheres.** VEGF-loaded and placebo microspheres were prepared with Symbiosys multiblock copolymers using a membrane emulsification-based double emulsion method and characterized as reported previously.<sup>35</sup> Microspheres were prepared with a 50:50 blend of Symbiosys multiblock copolymers A and B. Polymer A ( $\sim$ 54 kDa) consisted of 30 wt% of an amorphous, hydrophilic poly( $\epsilon$ -caprolactone)-PEG<sub>3000</sub>-poly( $\epsilon$ -caprolactone) (PCL-PEG<sub>3000</sub>-PCL) block with an  $M_w$  of 4000 g/mol and 70 wt% of a semi-crystalline poly(L-lactide) block with an  $M_w$  of 4000 g/mol. The total PEG weight fraction of polymer A is 22.5%. Polymer B ( $\sim$ 32 kDa) consisted of 50 wt% of PCL-PEG<sub>1000</sub>-PCL ( $M_w$  = 2000 g/mol) and 50 wt% of poly(L-lactide) block ( $M_w$  = 4000 g/mol), resulting in a PEG weight fraction of 25%. The total PEG content (%) of the 50:50 polymer blend is 23.8%. In brief, 1 mL of a solution of VEGF

(15–20 mg/mL in 5 mM sodium succinate buffer pH 5) was dispersed in a 10 mL of a multiblock copolymer solution (15–20 wt% in dichloromethane) by ultra-turrax homogenization (T25 Basic; IKA, Wilmington, NC; 40 s at 21,600 rpm). The resulting primary emulsion was pressed through 20  $\mu\text{m}$  pores of a stainless steel membrane (20  $\mu\text{m}$   $\times$  200  $\mu\text{m}$ ) hydrophilic ringed stainless steel membrane; Micropore Technologies, Redcar, UK into a continuous phase [4 wt% poly(vinyl alcohol), 5 wt% NaCl]. The secondary emulsion was stirred at 200 rpm with a magnetic stirrer for 3 h to evaporate the organic solvent. Obtained microspheres were collected on a 5  $\mu\text{m}$  filter and washed 3 times with water. After lyophilization, microspheres were stored at  $-20^\circ\text{C}$ . Nile Red-labeled placebo microspheres were prepared by membrane emulsification of a 10 wt% PLGA solution supplemented with 1 mg/mL Nile Red (conventional PLGA was used because these microspheres were only used for visual display of particle penetration within the devices). The average size distribution of the microspheres was measured with an optical particle sizer (Accusizer 780, Santa Barbara, CA). A size distribution plot is shown in [Figure S1](#).

**Preparation of Microsphere Dispersions in HA Carrier Liquid.** Microsphere dispersions in 1% HA carrier liquid were prepared by stirring a defined amount of microspheres in a corresponding amount of HA carrier liquid with a thin spatula until a homogeneous dispersion was obtained.

#### Characterization of PDMS Devices

**Scanning Electron Microscopy.** The surface morphology of the prepared PDMS devices was visualized by SEM. PDMS devices were submerged in deionized water and sonicated at  $37^\circ\text{C}$  3 times for 30 min to remove porogen (sodium chloride) crystals. Next, the devices were dried under vacuum at room temperature for 16 h. Slices of devices were cut with a razor blade and placed on stubs with double-sized carbon tape. The samples were coated with a thin platinum layer and imaged with SEM (Phenom; FEI Company, The Netherlands). The diameters of pores were measured with ImageJ (NIH, Bethesda, MD).

**Filling of PDMS Devices.** Dry devices were wetted and washed by submerging the devices in 20 mL deionized water and sonicating for 30 min at  $37^\circ\text{C}$  3 times. After each sonification step, the water was replaced. Freshly prepared solutions or microsphere dispersions in 1% HA carrier liquid (as described in sections [Release of Fluorescein, Blue Dextran, and FITC-HA Filled in PDMS Devices](#) and [Release of VEGF From Microspheres Filled in PDMS Devices](#)) were transferred into a 1 mL syringe. A target volume of 160  $\mu\text{L}$  was injected into prewetted devices via an 18G needle. The weight of the syringe and needle was noted before and after filling of the devices. The inlet of the device was closed with a custom-made stopper printed using FormLabs Form 2 Dental SG resin (FormLabs, Somerville, MA). Proper distribution of microspheres within the devices was visualized by filling with a 12 mg/mL dispersion of Nile Red-labeled microspheres in HA carrier liquid. Because Nile Red is not released from the microspheres, the red color in photographs represents the dispersion of microspheres within the lumen of the devices.

**HUVEC Live/Dead Biocompatibility Assay.** The toxicity of leachables from PDMS devices filled with HA carrier liquid was evaluated by a live/dead assay with HUVECs. Washed PDMS devices were filled with 160  $\mu\text{L}$  of HA carrier liquid (as described in the section [Filling of PDMS Devices](#), no microspheres present), transferred into a glass vial containing 10 mL of cell-compatible IVR buffer (Dulbecco's PBS pH 7.4, 0.2  $\mu\text{m}$  filtered, 0.5% bovine serum albumin, 30  $\mu\text{g}/\text{mL}$  gentamicin, and 15 ng/mL amphotericin) and incubated at  $37^\circ\text{C}$

under mild agitation. After 1, 2, 3, and 4 weeks of incubation, the complete supernatant was removed and replaced with fresh cell-compatible IVR buffer. The collected supernatants were diluted 20 times in HUVEC complete medium [endothelial cell basal medium 2 (C-22211) supplemented with endothelial cell growth medium 2 supplement mix (C-39216), both obtained from Sigma Aldrich]. Blank complete culture medium, cell-compatible IVR buffer diluted 20 times in complete medium, and 8  $\mu\text{g}/\text{mL}$  HA in complete medium containing 20 times diluted cell-compatible IVR buffer (which corresponds to the concentration of HA in filled devices) served as controls. Prior to the experiment, 96-well plates were coated overnight at  $4^\circ\text{C}$  with 100  $\mu\text{L}$  of collagen coating solution (50  $\mu\text{g}/\text{mL}$  collagen in 20 mM acidic acid). Afterward, plates were washed twice with PBS before seeding of the cells. Wells were filled with 100  $\mu\text{L}$  of sample or controls and 4000 cells suspended in 100  $\mu\text{L}$  of complete medium (200  $\mu\text{L}$  total volume per well). Cells were incubated at  $37^\circ\text{C}/5\%$   $\text{CO}_2$  for 24 h. Live/dead staining was made by incubating with Calcein AM and propidium iodide working solution (prepared according to the supplier's instructions) for 20 min. Images were taken with a fluorescent confocal microscope [Yokogawa Cell Voyager CV7000, Tokyo, Japan; Calcein AM (green signal):  $\lambda_{\text{ex}} = 490$  nm,  $\lambda_{\text{em}} = 515$  nm; propidium iodide (red signal):  $\lambda_{\text{ex}} = 535$  nm,  $\lambda_{\text{em}} = 617$  nm] and analyzed with Columbus image analysis software (PerkinElmer, Waltham, MA).

**Release of Fluorescein, Blue Dextran, and FITC-HA Filled in PDMS Devices.** A 1 mg/mL fluorescein solution was prepared by dissolving fluorescein sodium salt in 1% HA carrier liquid. Furthermore, 10 mg/mL solutions of Blue Dextran (~2 MDa) and FITC-labeled HA (1.26 MDa) were prepared by dissolving appropriate amounts of the compounds in PBS; the FITC-HA solution was gently heated ( $40^\circ\text{C}$ ) and stirred for 16 h to dissolve the polymer. The obtained solutions of fluorescein, Blue Dextran, and FITC-HA solutions were filled into PDMS devices as described in the section [Filling of PDMS Devices](#). Filled devices were transferred into a glass vial containing 10 mL of IVR buffer [consisting of Dulbecco's PBS pH 7.4 (0.2  $\mu\text{m}$  filtered), 0.025% Tween 20, 0.02%  $\text{NaN}_3$ ] and then incubated at  $37^\circ\text{C}$  under mild agitation. At appropriate time points, a 1 mL sample of the release medium was removed and replaced with fresh release buffer. The fluorescein or FITC-HA content in release samples was quantified by spectrofluorometry at  $\lambda_{\text{ex}} = 493$  nm and  $\lambda_{\text{em}} = 512$  nm using a Jasco spectrofluorometer FP-8300 (Jasco, Easton, MD). The Blue Dextran content in release samples was determined by UV spectroscopy at 620 nm using a SPECTROstar Nano plate reader (BMG Labtech, Ortenberg, Germany).

#### Rheological Measurements of Microsphere Dispersion

Microsphere dispersions of 6, 12, 20, 30, and 50 mg/mL were prepared essentially as described in the section [Preparation of Microsphere Dispersions in HA Carrier Liquid](#) and analyzed for their rheological properties using a Discovery HR-2 rheometer (TA Instruments, Etten-Leur, The Netherlands) equipped with a parallel plate measuring geometry (steel plate diameter = 40 mm). A shear stress ramp was obtained from 0.01 to 1 Pa at  $21^\circ\text{C}$ .

#### Release of VEGF From Microspheres Filled in PDMS Devices

Microsphere dispersions were prepared by weighing the appropriate amount of microspheres and suspending them in HA carrier liquid (final concentration 12 mg/mL, see the section [Preparation of Microsphere Dispersions in HA Carrier Liquid](#)) and filled into PDMS devices as described in the section [Filling of PDMS Devices](#). PDMS devices filled with VEGF-loaded microspheres were transferred into a glass vial containing 10 mL of IVR [consisting of Dulbecco's PBS pH 7.4 (0.2  $\mu\text{m}$  filtered), 0.025% Tween 20, 0.02%  $\text{NaN}_3$ ] and were then incubated at  $37^\circ\text{C}$  under mild agitation. At

appropriate time points, the complete release medium was removed and replaced with fresh IVR buffer. Released VEGF was quantified by a sandwich ELISA (Human VEGF DuoSet ELISA; R&D Systems, Abingdon, United Kingdom) according to the manufacturer's protocol. The VEGF stock solution of the ELISA kit was used for calibration in the concentration range of 31-2000 pg/mL. Release samples were diluted with reagent diluent to fall within the working range of the assay and measured in duplicate. ELISA plates were read at 450 nm using a SPECTROstar Nano plate reader (BMG Labtech).

Obtained VEGF release curves were fitted using the Korsmeyer-Peppas model, where  $Q_t$  is the amount of drug released from microspheres at time point  $t$ ,  $Q_0$  is the initial amount of drug in microspheres,  $n$  is diffusional exponent indicative of the transport mechanism, and  $K_p$  is Korsmeyer-Peppas constant incorporating structural and geometric characteristics of the dosage form (Eq. 1).<sup>42</sup> The diffusional exponent  $n$  was calculated from the fitted linear regression lines of  $\log(\% \text{ drug released})$  versus  $\log(\text{time})$  (Eq. 2). The obtained parameters of fitted VEGF release from microspheres filled in PDMS devices were compared to the parameters of the fit of the VEGF release curves from microspheres in IVR buffer, which have been reported previously.<sup>35</sup>

$$\frac{Q_t}{Q_0} = K_p \times t^n \quad (1)$$

Equation 1: Korsmeyer-Peppas equation

$$\log\left(\frac{Q_t}{Q_0}\right) = \log(K_p) + n \log(t) \quad (2)$$

Equation 2: adapted Korsmeyer-Peppas equation.

**Bioactivity of VEGF Released From PDMS Devices.** The bioactivity of released VEGF from the implants was analyzed by Alamar Blue proliferation assay with HUVECs, as described previously.<sup>35</sup> In short, a 12 mg/mL microsphere dispersion of VEGF-loaded microspheres in 1% HA carrier liquid was prepared as described in the section [Release of VEGF From Microspheres Filled in PDMS Devices](#) and filled in PDMS devices (see section [Filling of PDMS Devices](#)). Filled PDMS devices were incubated in 10 mL cell-compatible IVR buffer ("bioactivity IVR buffer"; Dulbecco's PBS pH 7.4, 0.2  $\mu\text{m}$  filtered, 0.5% bovine serum albumin, 30  $\mu\text{g}/\text{mL}$  gentamicin, and 15 ng/mL amphotericin) at 37°C under mild agitation. After 1, 2, 3, and 4 weeks of incubation, the complete release medium was removed and replaced by fresh bioactivity IVR buffer. Release samples were diluted in bioactivity medium to fall within the (linear) proliferation range of VEGF (0-20 ng/mL), corresponding to a relative cell proliferation of 1-3.5 (defined by the proliferation in % normalized by the proliferation of cells that were incubated without VEGF).

### Statistical Analysis

Data are presented as average with SD. Statistical analysis was performed with GraphPad Prism 7 using the one-way analysis of variance and Holm-Sidak multicomparison test. Differences between the analyzed groups were considered significant if  $p < 0.05$ .

## Results

### Characterization of PDMS Devices

**Figure 1a** shows a schematic image of the PDMS devices used in this study. PDMS devices were made by a 3-step printing process. First, 2 separately prepared membrane sheets were made from a PDMS/porogen mix which was subsequently crosslinked. Next, connecting support structures (PDMS, no porogen) were printed on

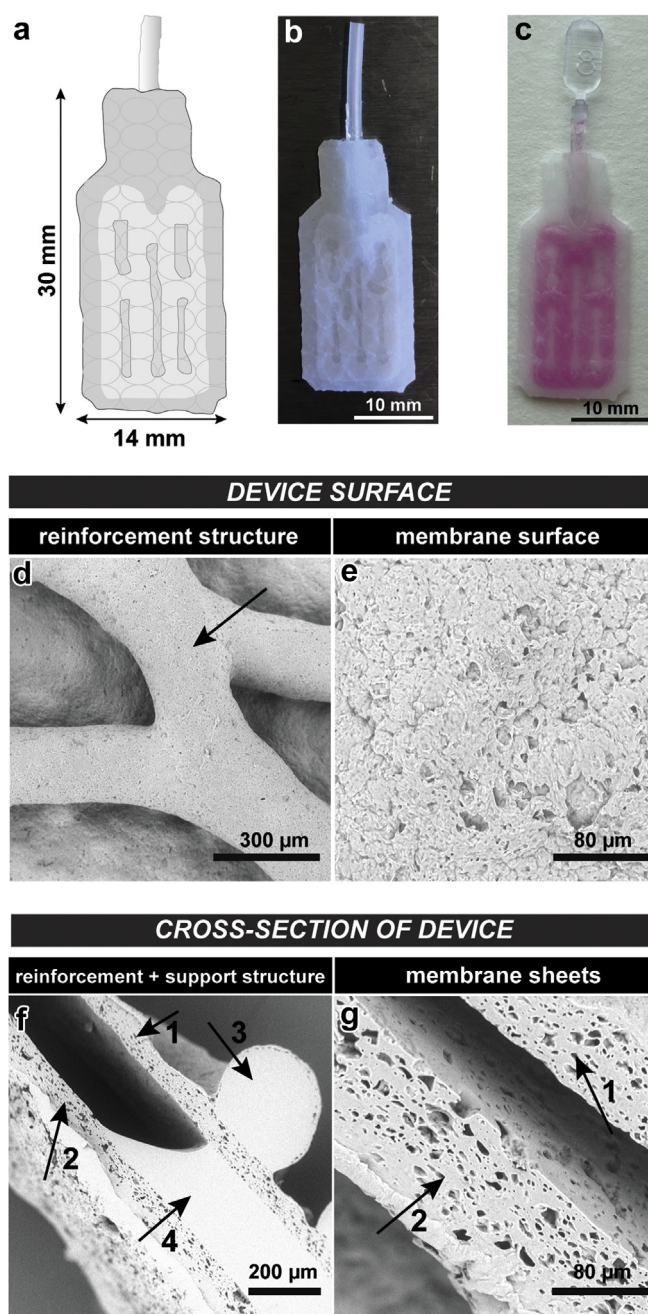


**Figure 1.** Imaging of PDMS devices (30 mm  $\times$  14 mm). (a) Schematic image of a PDMS device. (b) Photograph of a dry device with plastic inlet. (c) Photograph of a wetted device, filled with Nile Red-labeled microspheres (in pink). (d, e) SEM images of the device surface: (d) reinforcement structure on the outer surface of the device (indicated with arrow) and (e) membrane morphology of the outer surface of the device. (f, g) Cross-section of the device: (f) 2 membrane sheets (arrows 1 and 2), outer reinforcement structure (arrow 3), and support structure between 2 membrane sheets (arrow 4) and (g) close-up of 2 porous membrane sheets (arrows 1 and 2).

the outline and inner parts of one membrane (as shown in [Fig. 1b](#) in white). Then, a second membrane was placed on top of the support structures and the polymer was again crosslinked. Finally, reinforcement structures (PDMS) were printed on the 2 outer surfaces of the membranes and subsequently crosslinked. The dimensions of the printed devices were chosen for future use in rodent studies, aiming for subcutaneous implantation of the devices. Typically, the devices measured 30  $\times$  14  $\times$  0.8 mm, with an internal volume of  $\sim$ 160  $\mu\text{L}$  (active inner area of 20  $\times$  10  $\times$  0.8 mm). The surface

morphology of the biomaterial implants was created by 3D printing of a reinforcement structure of PDMS. Pores were introduced into the membranes by adding NaCl crystals (7–8  $\mu\text{m}$ ) as porogen to PDMS which were washed out with water after the printing process had been completed. Macroscopic pictures of the devices are shown in Figures 1b and 1c, whereby the distribution of microspheres within the inner lumen of the implants is visualized with Nile Red-labeled microspheres (as shown in reddish-pink color). The microspheres were distributed homogeneously in the accessible parts of the implants while support structures were not colored. The morphology of the 3D printed PDMS was analyzed by SEM (Figs 1d and 1e). Both surface and cross-sections of the device were selected. The reinforcement structures on the outside of the implants were smooth and  $\sim 300 \mu\text{m}$  thick (Fig. 1d). The outer surface of the membrane was smooth with a few pores (Fig. 1e). As seen in the cross-sections (Figs 1f and 1g), the inside of the implant was up to  $\sim 200 \mu\text{m}$  wide (Fig. 1f) and the membrane sheet had a porous network (pore sizes between 4 and 20  $\mu\text{m}$ ; Fig. 1g).

The release of possible toxic leachables was studied with devices filled with HA carrier liquid. Release supernatants were collected in weekly intervals up to 4 weeks of incubation, and did not show any sign of toxic effects (viability of HUVEC remained above 95% for all conditions), as shown in Figure S2.

Devices were filled with a fluorescein sodium solution in HA carrier liquid, to evaluate whether small molecules can permeate through the PDMS membrane. As shown in Figure 2 (yellow release curve), fluorescein was released completely within 2 h. In a similar setup, we evaluated the efflux of Blue Dextran ( $M_w$  of 2 MDa; blue release curve) and FITC-labeled HA ( $M_w$  of 1.26 MDa; orange release curve) from PDMS devices. Both polymers were released from the devices within 48 h with almost similar release kinetics.

#### Viscosity of Microsphere Dispersions in HA Carrier Liquid

In view of the final aim of loading pancreatic islets into the devices, it is crucial that dispersions of microspheres in HA carrier liquid can be injected into the PDMS devices via a 18G needle with only minimal injection force. We therefore investigated the rheological behavior of microsphere dispersions in HA carrier liquid with concentrations ranging from 6 to 50 mg/mL. As shown in Figure 3 (gray circles), 1% HA carrier liquid displayed a constant viscosity of 0.5 Pa·s at stresses ranging from 0.01 to 1.0 Pa, showing Newtonian rheological behavior (meaning that the viscosity is independent of the applied shear stress). On the other hand, dispersions of microspheres in HA carrier liquid showed shear-thinning behavior. The viscosity of dispersions of 6–20 mg/

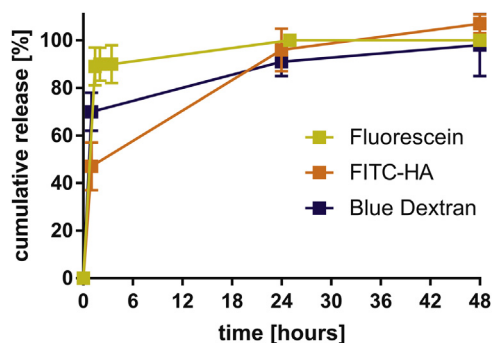


**Figure 2.** Cumulative release of fluorescein, FITC-HA, and Blue Dextran from PDMS devices. The devices were filled with a solution of fluorescein in HA carrier liquid, FITC-labeled HA (FITC-HA), or Blue Dextran in PBS, and were subsequently incubated at 37°C in IVR buffer.

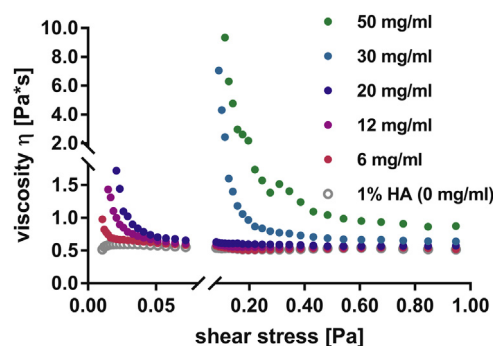


**Figure 3.** Rheological measurements of microsphere dispersions in 1% HA carrier liquid (concentrations of microspheres stated in mg/mL). Viscosities (y-axis) were measured using a shear stress ramp from 0.01 to 1.0 Pa (x-axis) at 21°C.

mL ranged from 1.0 to 1.7 Pa·s and decreased to about 0.5 Pa·s at shear stresses above 0.05 Pa. The microsphere dispersion of 30 mg/mL showed a decrease in viscosity from  $\sim 7.0 \text{ Pa}\cdot\text{s}$  to 0.5 Pa at shear stresses above 0.40 Pa. Similarly, the viscosity of 50 mg/mL microsphere dispersion decreased from  $\sim 9.0 \text{ Pa}\cdot\text{s}$  to  $\sim 1.0 \text{ Pa}\cdot\text{s}$  at shear stresses above 0.60 Pa. The yield stress, defined as the shear stress at which the microsphere dispersion starts to flow,<sup>43</sup> of dispersions at the tested concentrations (6–50 mg/mL) was relatively low, that is,  $<0.03 \text{ Pa}$  for 6–20 mg/mL and  $\sim 0.15 \text{ Pa}$  for 30 and 50 mg/mL, comparable to those of orange juice or blue ink.<sup>44</sup> We therefore conclude that all microsphere dispersions are easily injectable through an 18G needle.

#### Incorporation of VEGF Microspheres in Devices and VEGF Release

We selected 12 mg/mL as the preferred concentration of microspheres because at the loaded VEGF concentration and the inner volume of the devices, this would represent an appropriate theoretical dose of VEGF (i.e., 150 ng loaded VEGF, yielding an expected VEGF release of 5 ng/d, assuming continuous release of the loaded dose over 28 days<sup>35</sup>). Figure 4 shows that VEGF was released from PDMS devices throughout the release period of 28 days in a similar pattern as VEGF release measured from microspheres in suspension as published previously.<sup>35</sup> Indeed, the diffusional exponent for microspheres filled in devices ( $0.43 \pm 0.03$ ) was comparable to the diffusional exponent of  $0.41 \pm 0.02$  for microspheres in suspension, as derived from nonexponential fitting by the Korsmeyer-Peppas model<sup>42,45</sup> (Table 1).

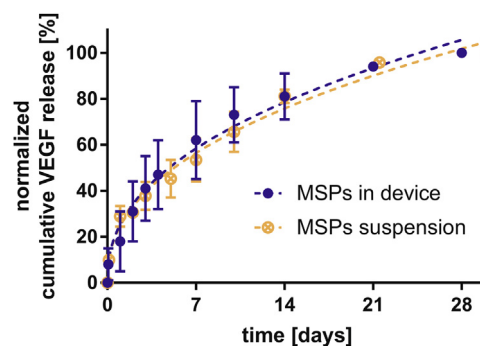


**Figure 4.** Normalized cumulative release (%) of VEGF from PDMS devices filled with VEGF-loaded microspheres (blue curve) and VEGF-loaded microspheres in suspension (orange curve, adapted from Scheiner et al.,<sup>35</sup> ACS Omega). Release experiments were performed in IVR buffer at 37°C ( $n = 3$ , shown as average  $\pm$  SD). Released VEGF was quantified by ELISA and normalized to 100% based on the total release observed under the test conditions. MSP, microspheres.

### Bioactivity of VEGF Released From PDMS Devices

The bioactivity of VEGF released from the PDMS devices was assessed with an HUVEC proliferation assay. As shown in Figure 5, endothelial cell proliferation was stimulated up to 3-fold by spiked VEGF samples in the dose range of 0.5–20 ng/mL (see Fig. S3 for a detailed calibration curve of VEGF). IVR samples of all time points, diluted 20 or 100×, stimulated endothelial cell proliferation between 1.5- and 3-fold in a dose-dependent manner corresponding to the expected concentrations of 2–10 ng/mL (for 100-fold and 20-fold diluted samples, respectively). Importantly, Figure 5 confirms that bioactive VEGF was released during the full 4-week timespan of the release study. Control experiments with PDMS devices filled with placebo microspheres did not stimulate endothelial cell proliferation.

### Discussion

The aim of this study is to develop an *in vitro* prevascularization strategy of PDMS devices by incorporating microspheres that release VEGF, the most prominent proangiogenic growth factor.<sup>46</sup> These microspheres have demonstrated continuous VEGF release for 4 weeks,<sup>35</sup> which has been shown to be a favorable release window for implant vascularization.<sup>47,48</sup> Devices used in this study were prepared with PDMS, a polymer that has been well-studied for its application for pancreatic islet transplantation due to its bioinertness and biocompatibility.<sup>39,49,50</sup> SEM revealed a porous network within the PDMS membrane which is needed for efficient in and out diffusion of nutrients and proteins.<sup>51,52</sup> Indeed, the permeability of the membrane was demonstrated by complete release of fluorescein, FITC-labeled HA, and Blue Dextran from PDMS implant within 48 h. Hence, we do not expect a significant barrier function for nutrients and other small molecules that need to diffuse from biological fluids into and from the device upon transplantation. Furthermore, our results show biocompatibility of PDMS devices, in line with previous studies.<sup>53,54</sup> The rheological measurements of microsphere dispersions with concentrations ranging from 6 to 50 mg/mL revealed low yield pressures and thus excellent syringeability for filling-in PDMS devices. VEGF-loaded microspheres filled in PDMS devices showed sustained release of this protein for 4 weeks. Figure 4 shows that the devices had the same release characteristics as the microspheres suspended in buffer, that is, diffusion-controlled release (see Table 1) through a water-filled porous network within the polymeric matrix of the microspheres, caused by the hydrophilic PEG of the multiblock copolymers.<sup>35</sup> This means that VEGF release from the devices is neither controlled by diffusion over the PDMS membrane nor binding to PDMS, and it is primarily controlled by its release from the microspheres. This is not surprising as the diameters of membrane pores (as visible by SEM; Fig. 1) created by salt leaching are much bigger than the hydrodynamic radius of VEGF and Blue

**Table 1**

Korsmeyer-Peppas Model Fit Parameters for Normalized Cumulative VEGF Release Curves Measured by ELISA of Microspheres in Suspension and Incorporated in PDMS Devices, as Shown in Figure 4 as Orange and Blue Dotted Lines, Respectively

Parameters	VEGF Release Quantified by ELISA	
	MSP Suspension	MSP in Device
<i>n</i>	0.41 ± 0.02	0.43 ± 0.03
95% CI	0.37–0.44	0.37–0.49
<i>R</i> <sup>2</sup>	0.97	0.91

*n*, diffusional exponent; 95% CI, 95% confidence interval; *R*<sup>2</sup>, correlation coefficient; MSP, microspheres.

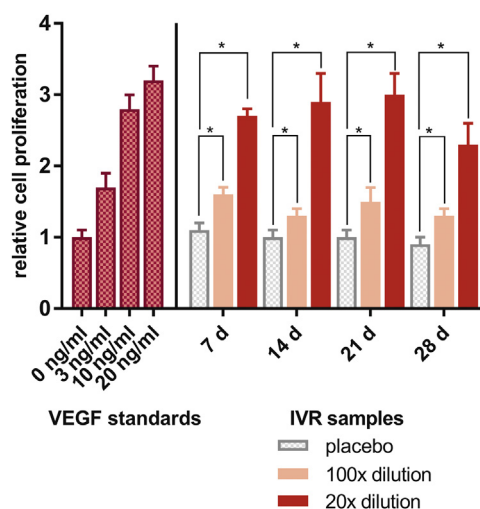


**Figure 5.** Bioactivity of VEGF released from PDMS devices filled with VEGF-loaded microspheres. On the left side of the graph: pink bars represent linear responsive range of VEGF standards between 0 and 20 ng/mL. On the right side of the graph (gray, light red, and red bars): relative cell proliferation of released VEGF (“IVR samples”) from PDMS devices filled with VEGF-loaded microspheres per time point. IVR supernatants were diluted 100× (light red bars) and 20× (red bars). IVR supernatants of devices filled with placebo microspheres served as controls (gray bars: placebo). The release study was performed in cell-compatible “bioactivity IVR buffer” without sodium azide and Tween 20 at 37°C. Bars represent average ± SD of *n* = 3. \**p* < 0.05, 100× dilution or 20× dilution versus placebo IVR samples.

Dextran ( $R_H \sim 27$  nm<sup>55</sup>). Importantly, VEGF was released in its bioactive form from microspheres loaded in PDMS devices. The released amount, based on the chosen microsphere concentration (12 mg/mL) and release of bioactive VEGF (Fig. 5), is considered optimal for sufficient vascularization and thus performance of biomaterial implants, that is, 150 ng/0.1 mL implant for 4 weeks.<sup>15,25</sup> Although it is known that VEGF is well suitable for vascularization of biomaterial implants,<sup>11–13</sup> angiogenesis *in vivo* is an interplay of several different growth factors and cytokines, such as fibroblast growth factor, hepatocyte growth factor, and platelet-derived growth factor, besides VEGF.<sup>16,56</sup> Polymeric microspheres offer the possibility to encapsulate and release other growth factors as well, and these microspheres can also be incorporated in biomaterial devices intended for implantation *in vivo*, such as PDMS devices used in this study.

In future *in vivo* studies, we aim to investigate the suitability for this device design for pancreatic islet transplantation in a rodent diabetes model. Two options are possible for integrating pancreatic islets with the vascularization approach of this study. Our current work has focused on developing a protocol for mixing rat pancreatic islets with VEGF-loaded microspheres in an HA-based suspension and subsequently filling this suspension in PDMS devices. Besides this, a prevascularization approach also seems feasible, where PDMS devices are first filled with VEGF-loaded microsphere suspension and implanted subcutaneously in rats. After 4 weeks, pancreatic islets can then be added into the (vascularized) PDMS device via the inlet. For both options, the compatibility of pancreatic islets with VEGF and VEGF-loaded microspheres needs to be ensured and is therefore part of our current investigations.

### Conclusion

In this study, we have incorporated VEGF-releasing microspheres in PDMS-based devices using 1% HA solution as carrier liquid. PDMS devices, created with salt leaching and 3D printing,

showed a porous network and high permeability of fluorescein, FITC-labeled HA, and Blue Dextran. PDMS devices filled with HA carrier liquid showed cytocompatibility with endothelial cells. Microsphere dispersions of various concentrations in HA carrier liquid showed good syringeability. VEGF was released continuously from PDMS devices for 4 weeks, with release kinetics comparable to microspheres in suspension in buffer. The release of VEGF from PDMS devices is therefore governed by the microspheres, as no significant delay by the PDMS membrane was observed. Released VEGF from PDMS devices remained bioactive over the entire release period of 4 weeks. In conclusion, PDMS devices functionalized with VEGF-releasing microspheres are an attractive vascularization strategy for pancreatic islet-filled implants, which will be studied in future *in vivo* studies.

## Acknowledgments

This work was supported by European Union's Horizon 2020 research and innovation program "Diabetes-Reversing Implants for enhanced Viability and long-term Efficacy" (DRIVE) [grant agreement number 645991]. The authors would like to thank Marcel Fens, Cedric Hustinx, Johanna Walther, Joep van den Dikkenberg, and Mies van Steenberghe for their excellent practical assistance. Contipro (Prague, Czech Republic) is acknowledged for providing hyaluronic acid.

## References

- Richardson SJ, Morgan NG, Foulis AK. Pancreatic pathology in type 1 diabetes mellitus. *Endocr Pathol*. 2014;25(1):80-92.
- Shapiro AM, Pokrywczynska M, Ricordi C. Clinical pancreatic islet transplantation. *Nat Rev Endocrinol*. 2017;13(5):268-277.
- Khosravi-Maharlooie M, Hajizadeh-Saffar E, Tahamtani Y, et al. Therapy of endocrine disease: islet transplantation for type 1 diabetes: so close and yet so far away. *Eur J Endocrinol*. 2015;173(5):R165-R183.
- Shapiro AM, Lakey JR, Ryan EA, et al. Islet transplantation in seven patients with type 1 diabetes mellitus using a glucocorticoid-free immunosuppressive regimen. *N Engl J Med*. 2000;343(4):230-238.
- Desai T, Shea LD. Advances in islet encapsulation technologies. *Nat Rev Drug Discov*. 2017;16(5):338-350.
- Canibano-Hernandez A, Saenz Del Burgo L, Espona-Noguera A, Ciriza J, Pedraz JL. Current advanced therapy cell-based medicinal products for type-1 diabetes treatment. *Int J Pharm*. 2018;543(1-2):107-120.
- Dimitrioglou N, Kanelli M, Papageorgiou E, Karatzas T, Hatzivramidis D. Paving the way for successful islet encapsulation. *Drug Discov Today*. 2019;24(3):737-748.
- Uematsu SS, Inagaki A, Nakamura Y, et al. The optimization of the pre-vascularization procedures for improving subcutaneous islet engraftment. *Transplantation*. 2018;102(3):387-395.
- Farina M, Chua CYX, Ballerini A, et al. Transcutaneously refillable, 3D-printed biopolymeric encapsulation system for the transplantation of endocrine cells. *Biomaterials*. 2018;177:125-138.
- Smink AM, Li S, Hertsig DT, et al. The efficacy of a prevascularized, retrievable poly(D,L-lactide-co-epsilon-caprolactone) subcutaneous scaffold as transplantation site for pancreatic islets. *Transplantation*. 2017;101(4):e112-e119.
- Wagner ER, Parry J, Dadsetan M, et al. VEGF-mediated angiogenesis and vascularization of a fumarate-crosslinked polycaprolactone (PCLF) scaffold. *Connect Tissue Res*. 2018;59(6):542-549.
- Quinlan E, Lopez-Noriega A, Thompson EM, Hibbitts A, Cryan SA, O'Brien FJ. Controlled release of vascular endothelial growth factor from spray-dried alginate microparticles in collagen-hydroxyapatite scaffolds for promoting vascularization and bone repair. *J Tissue Eng Regen Med*. 2017;11(4):1097-1109.
- Farina M, Ballerini A, Fraga DW, et al. 3D printed vascularized device for subcutaneous transplantation of human islets. *Biotechnol J*. 2017;12(9). <https://doi.org/10.1002/biot.201700169>.
- Silva EA, Mooney DJ. Effects of VEGF temporal and spatial presentation on angiogenesis. *Biomaterials*. 2010;31(6):1235-1241.
- Davies N, Dobner S, Bezuidenhout D, et al. The dosage dependence of VEGF stimulation on scaffold neovascularisation. *Biomaterials*. 2008;29(26):3531-3538.
- Said SS, Pickering JG, Mequanint K. Advances in growth factor delivery for therapeutic angiogenesis. *J Vasc Res*. 2013;50(1):35-51.
- Lee K, Silva EA, Mooney DJ. Growth factor delivery-based tissue engineering: general approaches and a review of recent developments. *J R Soc Interface*. 2011;8(55):153-170.
- Giteau A, Venier-Julienne MC, Aubert-Pouessel A, Benoit JP. How to achieve sustained and complete protein release from PLGA-based microparticles? *Int J Pharm*. 2008;350(1-2):14-26.
- Ma G. Microencapsulation of protein drugs for drug delivery: strategy, preparation, and applications. *J Control Release*. 2014;193:324-340.
- Rui J, Dadsetan M, Runge MB, et al. Controlled release of vascular endothelial growth factor using poly-lactic-co-glycolic acid microspheres: in vitro characterization and application in polycaprolactone fumarate nerve conduits. *Acta Biomater*. 2012;8(2):511-518.
- van de Weert M, Hennink WE, Jiskoot W. Protein instability in poly(lactic-co-glycolic acid) microparticles. *Pharm Res*. 2000;17(10):1159-1167.
- Schwendeman SP. Recent advances in the stabilization of proteins encapsulated in injectable PLGA delivery systems. *Crit Rev Ther Drug Carrier Syst*. 2002;19(1):73-98.
- Simon-Yarza T, Tamayo E, Benavides C, et al. Functional benefits of PLGA particulates carrying VEGF and CoQ10 in an animal of myocardial ischemia. *Int J Pharm*. 2013;454(2):784-790.
- Simon-Yarza T, Formiga FR, Tamayo E, Pelacho B, Prosper F, Blanco-Prieto MJ. PEGylated-PLGA microparticles containing VEGF for long term drug delivery. *Int J Pharm*. 2013;440(1):13-18.
- Amsden BG, Timbart L, Marecak D, Chapanian R, Tse MY, Pang SC. VEGF-induced angiogenesis following localized delivery via injectable, low viscosity poly(trimethylene carbonate). *J Control Release*. 2010;145(2):109-115.
- Fu K, Pack DW, Klibanov AM, Langer R. Visual evidence of acidic environment within degrading poly(lactic-co-glycolic acid) (PLGA) microspheres. *Pharm Res*. 2000;17(1):100-106.
- Shenderova A, Burke TG, Schwendeman SP. The acidic microclimate in poly(lactide-co-glycolide) microspheres stabilizes camptothecins. *Pharm Res*. 1999;16(2):241-248.
- Giteau A, Venier-Julienne MC, Marchal S, et al. Reversible protein precipitation to ensure stability during encapsulation within PLGA microspheres. *Eur J Pharm Biopharm*. 2008;70(1):127-136.
- Estey T, Kang J, Schwendeman SP, Carpenter JF. BSA degradation under acidic conditions: a model for protein instability during release from PLGA delivery systems. *J Pharm Sci*. 2006;95(7):1626-1639.
- Kissel T, Li Y, Unger F. ABA-triblock copolymers from biodegradable polyester A-blocks and hydrophilic poly(ethylene oxide) B-blocks as a candidate for in situ forming hydrogel delivery systems for proteins. *Adv Drug Deliv Rev*. 2002;54(1):99-134.
- Bonacucina G, Cespi M, Mencarelli G, Giorgioni G, Palmieri GF. Thermosensitive self-assembling block copolymers as drug delivery systems. *Polymers-Basel*. 2011;3(2):779-811.
- Stankovic M, Hiemstra C, de Waard H, et al. Protein release from water-swelling poly(D,L-lactide-PEG)-b-poly(-caprolactone) implants. *Int J Pharm*. 2015;480(1-2):73-83.
- Stankovic M, Tomar J, Hiemstra C, Steendam R, Frijlink HW, Hinrichs WL. Tailored protein release from biodegradable poly(epsilon-caprolactone-PEG)-b-poly(epsilon-caprolactone) multiblock-copolymer implants. *Eur J Pharm Biopharm*. 2014;87(2):329-337.
- Teekamp N, Van Dijk F, Broesder A, et al. Polymeric microspheres for the sustained release of a protein-based drug carrier targeting the PDGFbeta-receptor in the fibrotic kidney. *Int J Pharm*. 2017;534(1-2):229-236.
- Scheiner KC, Maas-Bakker RF, Nguyen TT, et al. Sustained release of vascular endothelial growth factor from poly(epsilon-caprolactone-PEG-epsilon-caprolactone)-b-poly(L-lactide) multiblock copolymer microspheres. *ACS Omega*. 2019;4(7):11481-11492.
- Sandker MJ, Duque LF, Redout EM, et al. Degradation, intra-articular retention and biocompatibility of monospheres composed of [PDLLA-PEG-PDLLA]-b-PLLA multi-block copolymers. *Acta Biomater*. 2017;48:401-414.
- European Patent Office. European Patent Application EP 3409239A1 an implantable active agent encapsulating device. Available at: <https://patentimages.storage.googleapis.com/f9/33/95/6517ae214da3fe/EP3409239A1.pdf>. Accessed August 15, 2019.
- Harrington S, Williams J, Rawal S, Ramachandran K, Stehno-Bittel L. Hyaluronic acid/collagen hydrogel as an alternative to alginate for long-term immunoprotected islet transplantation. *Tissue Eng A*. 2017;23(19-20):1088-1099.
- Pedraza E, Brady AC, Fraker CA, et al. Macroporous three-dimensional PDMS scaffolds for extrahepatic islet transplantation. *Cell Transplant*. 2013;22(7):1123-1135.
- Shrestha P, Regmi S, Jeong J-H. Injectable hydrogels for islet transplantation: a concise review. *J Pharm Invest*. 2019. <https://doi.org/10.1007/s40005-019-00433-3>.
- Chia HN, Wu BM. Recent advances in 3D printing of biomaterials. *J Biol Eng*. 2015;9:4.
- Ritger PL, Peppas NA. A simple equation for description of solute release II. Fickian and anomalous release from swellable devices. *J Control Release*. 1987;5:37-42.
- Mouser VH, Melchels FP, Visser J, Dhert WJ, Gawlitta D, Malda J. Yield stress determines bioprintability of hydrogels based on gelatin-methacryloyl and gellan gum for cartilage bioprinting. *Biofabrication*. 2016;8(3):035003.
- TA instruments. Rheological techniques for yield stress analysis. Available at: <https://www.tainstruments.com/pdf/literature/RH025.pdf>. Accessed August 15, 2019.
- Costa P, Sousa Lobo JM. Modeling and comparison of dissolution profiles. *Eur J Pharm Sci*. 2001;13(2):123-133.
- Yla-Herttuala S, Rissanen TT, Vajanto I, Hartikainen J. Vascular endothelial growth factors: biology and current status of clinical applications in cardiovascular medicine. *J Am Coll Cardiol*. 2007;49(10):1015-1026.
- Rouwkema J, Rivron NC, van Blitterswijk CA. Vascularization in tissue engineering. *Trends Biotechnol*. 2008;26(8):434-441.

48. Cao L, Mooney DJ. Spatiotemporal control over growth factor signaling for therapeutic neovascularization. *Adv Drug Deliv Rev.* 2007;59(13):1340-1350.
49. Abbasi F, Mirzadeh H, Katbab A-A. Modification of polysiloxane polymers for biomedical applications: a review. *Polym Int.* 2001;50(12):1279-1287.
50. Blanco I. Polysiloxanes in theranostics and drug delivery: a review. *Polymers (Basel).* 2018;10(7):755.
51. Brauker JH, Carr-Brendel VE, Martinson LA, Crudele J, Johnston WD, Johnson RC. Neovascularization of synthetic membranes directed by membrane microarchitecture. *J Biomed Mater Res.* 1995;29(12):1517-1524.
52. Colton CK. Oxygen supply to encapsulated therapeutic cells. *Adv Drug Deliv Rev.* 2014;67-68:93-110.
53. Laffleur F, Netsomboon K, Erman L, Partenhauser A. Evaluation of modified hyaluronic acid in terms of rheology, enzymatic degradation and mucoadhesion. *Int J Biol Macromol.* 2019;123:1204-1210.
54. Sivarapatna A, Ghaedi M, Xiao Y, et al. Engineered microvasculature in PDMS networks using endothelial cells derived from human induced pluripotent stem cells. *Cell Transplant.* 2017;26(8):1365-1379.
55. Armstrong JK, Wenby RB, Meiselman HJ, Fisher TC. The hydrodynamic radii of macromolecules and their effect on red blood cell aggregation. *Biophys J.* 2004;87(6):4259-4270.
56. Novosel EC, Kleinhans C, Kluger PJ. Vascularization is the key challenge in tissue engineering. *Adv Drug Deliv Rev.* 2011;63(4-5):300-311.